

Supplementary information for

**New Imaging Reagents for Lipid Dense Region in
Live cells and Nucleus in Fixed MCF-7 cells**

Vadde Ramu,^a Firoj Ali,^a Nandaraj Taye,^b Bikash Garai,^a Aftab Alam,^b Samit Chattopadhyay,^{b*} Amitava Das^{a*}

^aCSIR-National Chemical Laboratory, Organic Chemistry Division, Pune - 411008, India, Email: a.das@ncl.res.in; Tel: +91(0)20 2590 2385; Fax: +91(0)20 2590 2629.

^bChromatin and Disease Biology Lab; National Centre for Cell Science; Pune - 411007, India, Email: samit@nccs.res.in.

Table of contents:	Page No.
Synthetic scheme	S3
Details of crystal structures of complex 1	S3-S5
Life time studies of 1, 2, 3 and absorbance spectra for 3	S6
Absorbance and emission spectra of compound 3 recorded in water	S6
Partition coefficient measurements (logP)	S6
Isothermal Titration Calorimetry (ITC) studies	S7
MTT assay results	S7
Viscosity measurement	S8
Cellular uptake quantification of 1, 2 and 3 by MP-AES.	S8
¹ H, ¹⁹ F-NMR and Mass spectra of L ₁ and L ₂	S9-S13
¹ H, ¹⁹ F NMR and HRMS spectra of complex 1 and 2	S13-S19
¹ H NMR and LCMS spectra for 3	S19-S20
Live MCF-7 cells incubated with 1 and 2 at 4°C for 4h	S21
CLSM images of fixed MCF-7 cells stained with 1 and 2 without DAPI	S21
References	S21

Synthetic scheme:

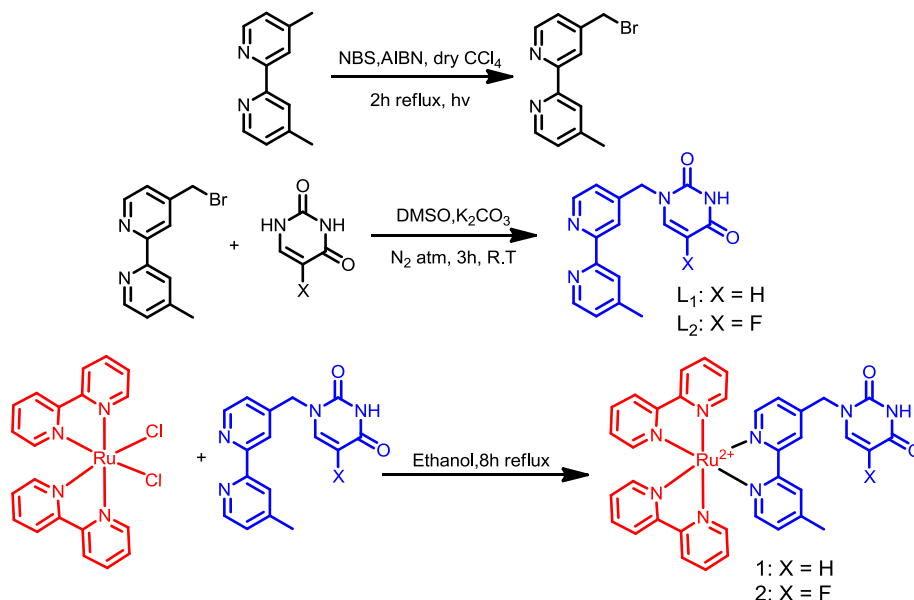


Figure S1. Synthetic methodology for the preparation of complexes **1** and **2**.

Single crystal X-Ray diffraction studies and crystal structures of complex 1:

As-synthesized crystal of complex **2** was coated with paratone-N and placed on top of a nylon cryoloop (Hampton research) and then mounted in the diffractometer. The data collection was done at 298 K. The crystal was mounted on a Super Nova Dual source X-ray diffractometer system (Agilent Technologies) equipped with a CCD area detector and operated at 250 W power (50 kV, 0.8 mA) to generate Mo $\text{K}\alpha$ radiation ($\lambda = 0.71073 \text{ \AA}$) and Cu $\text{K}\alpha$ radiation ($\lambda = 1.54178 \text{ \AA}$) at 298 K. Initial scans of each specimen were performed to obtain preliminary unit cell parameters and to assess the mosaicity (breadth of spots between frames) of the crystal to select the required frame width for data collection. CrysAlis^{Pro} program software was used suite to carry out overlapping φ and ω scans at detector (2θ) settings ($2\theta = 28$). Following data collection, reflections were sampled from all regions of the Ewald sphere to redetermine unit cell parameters for data integration. In no data collection was evidence for crystal decay encountered. Following exhaustive review of collected frames the resolution of the dataset was judged. Data were integrated using CrysAlis^{Pro} software with a narrow frame algorithm. Data were subsequently corrected for absorption by the program SCALE3 ABSPACK¹ scaling algorithm. These structures were solved by direct method and refined using the SHELXTL 97² software suite. Atoms were located from iterative examination of difference F-maps following least

squares refinements of the earlier models. Final model was refined anisotropically (if the number of data permitted) until full convergence was achieved. Hydrogen atoms were placed in calculated positions ($C-H = 0.93 \text{ \AA}$) and included as riding atoms with isotropic displacement parameters 1.2-1.5 times U_{eq} of the attached C atoms. In some cases modeling of electron density within the voids of the frameworks did not lead to identification of recognizable solvent molecules in these structures, probably due to the highly disordered contents of the large pores in the frameworks. Highly porous crystals that contain solvent-filled pores often yield raw data where observed strong (high intensity) scattering becomes limited to $\sim 1.0 \text{ \AA}$ at best, with higher resolution data present at low intensity. A common strategy for improving X-ray data, increasing the exposure time of the crystal to X-rays, did not improve the quality of the high angle data in this case, as the intensity from low angle data saturated the detector and minimal improvement in the high angle data was achieved. Additionally, diffused scattering from the highly disordered solvent within the void spaces of the framework and from the capillary to mount the crystal contributes to the background and the ‘washing out’ of the weaker data. Electron density within void spaces has not been assigned to any guest entity but has been modeled as isolated oxygen and/or carbon atoms. The foremost errors in all the models are thought to lie in the assignment of guest electron density. The structure was examined using the *ADSYM* subroutine of PLATON³ to assure that no additional symmetry could be applied to the models. The ellipsoids in ORTEP diagrams are displayed at the 50% probability level.

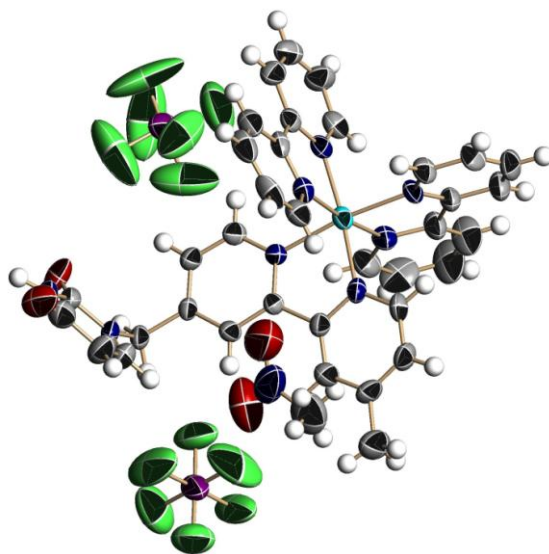


Figure S2. X-ray structure of complex 1. Thermal ellipsoids set to 50% probability level.

Table S1: Crystal structure and refinement details of 1

Empirical formula	C37 H33 F12 N9 O4 P2 Ru
Formula weight	1058.73
Temperature	298 K
Wavelength	0.71073 Å
Crystal system	Monoclinic
Space group	<i>C</i> 2/ <i>c</i>
Unit cell dimensions	$a = 39.898(4)$ Å $\alpha = 90^\circ$ $b = 10.0280(8)$ Å $\beta = 107^\circ$ $c = 22.1207(14)$ Å $\gamma = 90^\circ$
Unit cell volume	8462.4(13)
Z	8
Density (calculated)	1.662 mg mm ⁻³
Absorption coefficient	0.551
F(000)	4256
Crystal size	0.3 × 0.2 × 0.2 mm ³
Theta range for data collection	2.95 to 29.14
Index ranges	-51 ≤ h ≤ 53, -13 ≤ k ≤ 13, -27 ≤ l ≤ 29
Reflections collected	23879
Independent reflections	22963
Absorption correction	Semi-empirical from equivalents
Refinement method	Full-matrix least-squares on F ²
Data / restraints / parameters	9749/0/587
Goodness-of-fit on F ²	1.606
Final R indices [I ≥ 2σ(I)]	R ₁ = 0.0812, wR ₂ = 0.1504
R indices (all data)	R ₁ = 0.1609, wR ₂ = 0.1662
Largest diff. peak and hole	0.841 and -0.626 e.Å ⁻³
CCDC No	1035338

Lifetime studies:

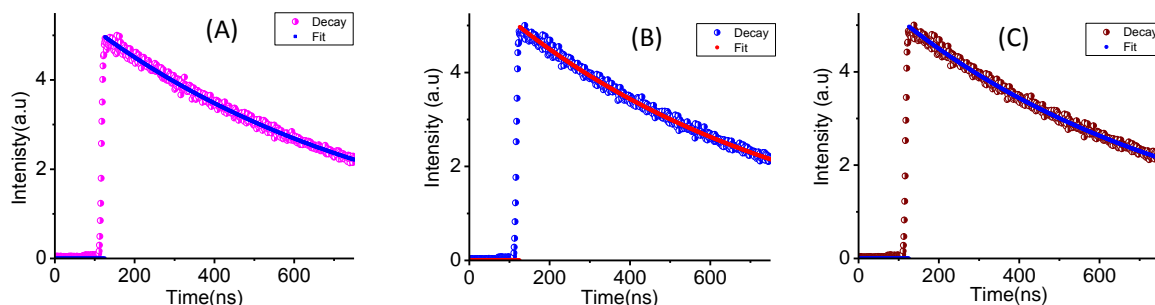


Figure S3. Fluorescence life time decay for the complex **1**(A) **2**(B) and **3**(C) fitted with single exponential. Time correlated single photon counting studies (TCSPC) were performed in aqueous medium. Excitation source: 443nm laser.

Absorbance and emission spectra for compound 3.

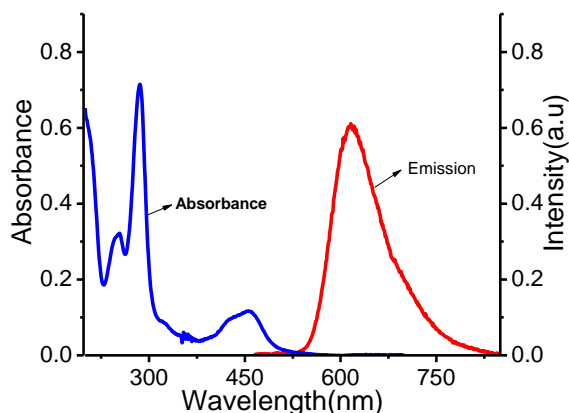


Figure S4. Absorbance and emission spectra of compound **3** recorded in water.

Table S2. LogP values obtained using shake-flask method. Molinspiration software was used for calculation of logP values for uracil and 5-FU. (<http://www.molinspiration.com/cgi-bin/properties>).

Compound	1	2	3	Uracil	5-Fluorouracil
LogP	-0.89± 0.05	-0.50± 0.02	-1.01±0.04	-0.89	-0.58

Isothermal Titration Calorimetry (ITC) studies:

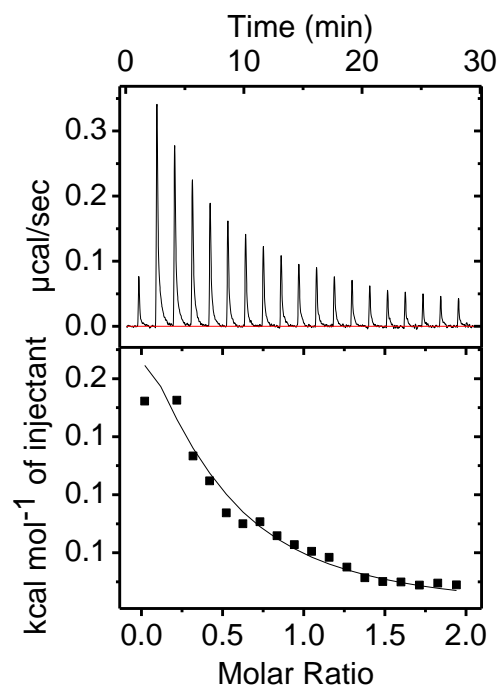


Figure S4. ITC binding profile for the interaction for complex **3** with CT-DNA.

MTT assays:

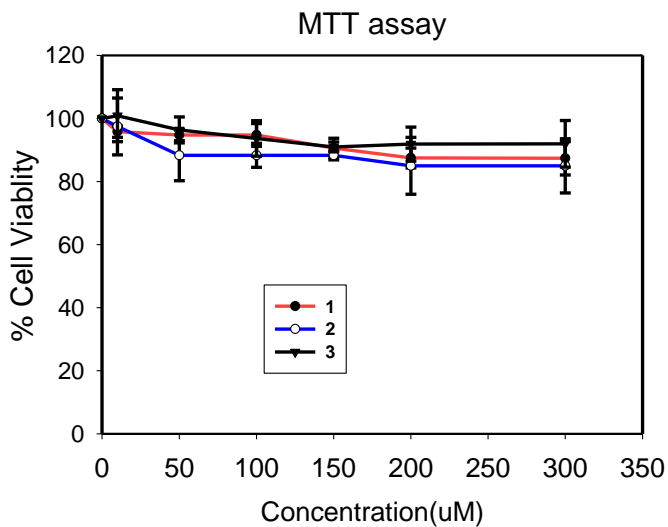


Figure S5. Cell viability assay of complexes **1**, **2**, and **3** on MCF-7 cells.

Viscosity measurements:

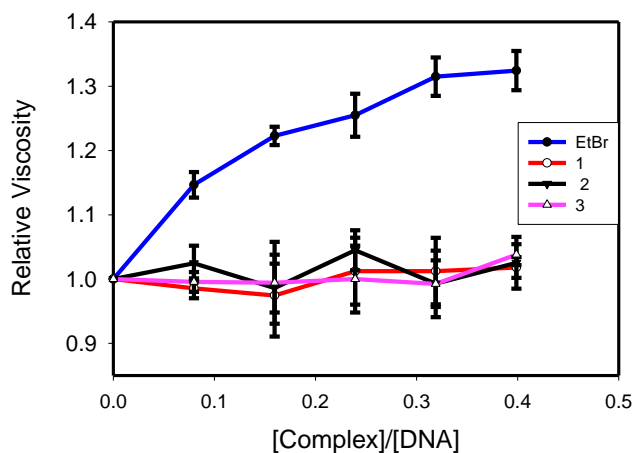


Figure S6. Change in the relative viscosity of CT-DNA by addition of complexes **1**, **2**, **3**, and Ethidium bromide.

Cellular uptake quantification by MP-AES:

Table S3. LogP measurements and the cellular accumulation values of **1**, **2**, and **3**.

Complex	logP	Ru accumulation ppm /10 ⁶ cells
1	-0.85	1.5
2	-0.50	2.3
3	-1.1	0.8

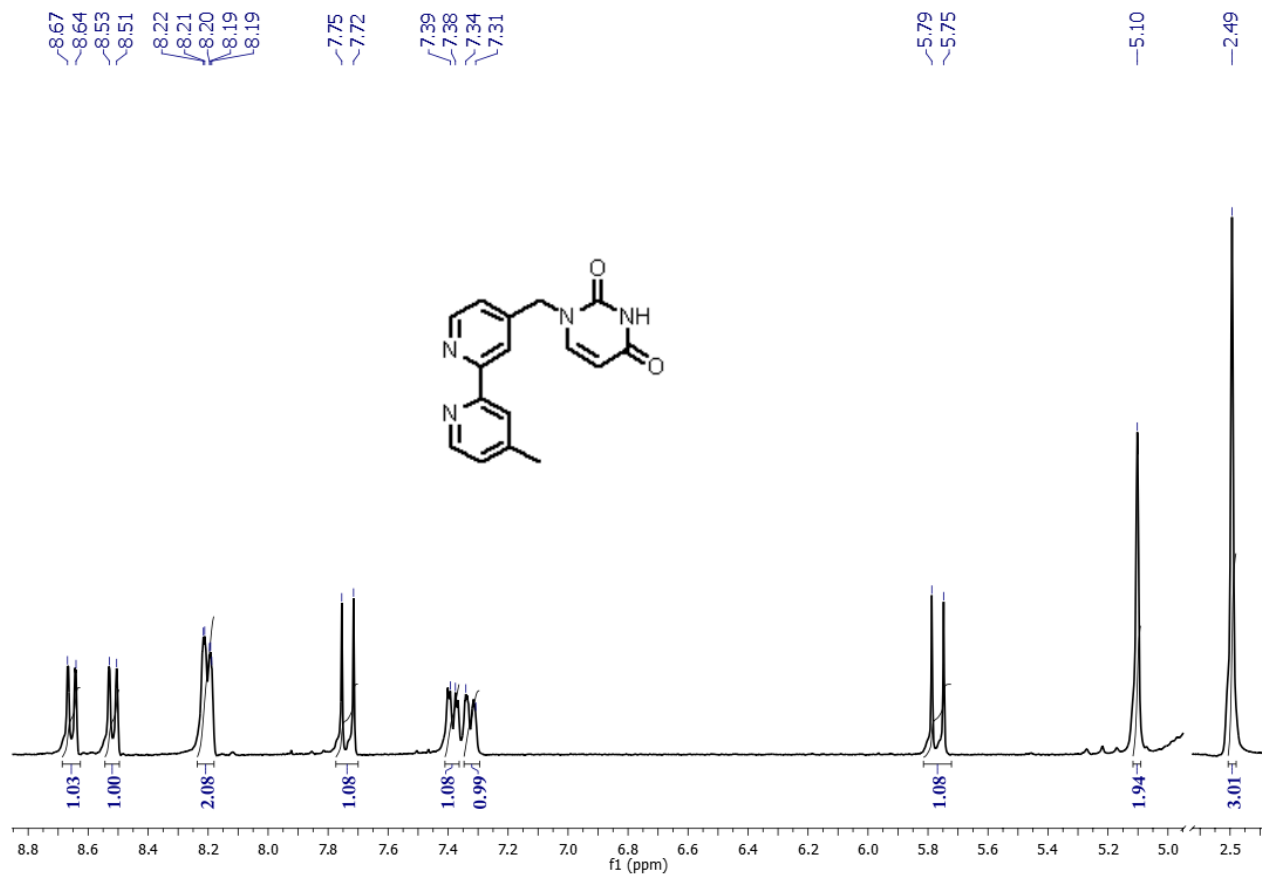


Figure S7. ¹H NMR spectra of the ligand L₁ in methanol-d₄.

VRB2-31 #9-21 RT: 0.14-0.35 AV: 13 SB: 37 0.00-0.14 , 0.38-0.85 NL: 2.74E6
T: {0,0} + c ESI corona sid=75.00 det=1000.00 Full ms [100.00-2000.00]

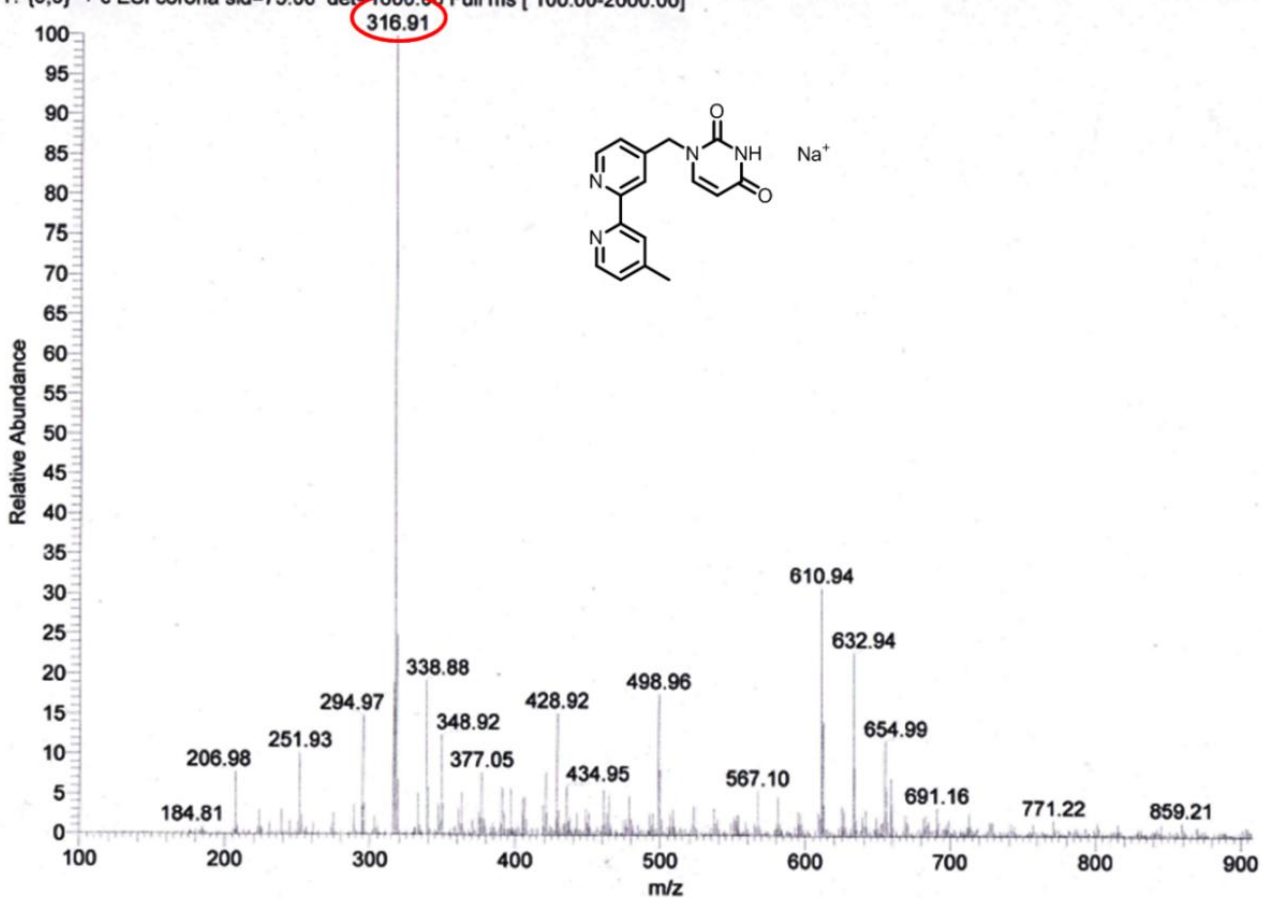


Figure S8. ESI-mass spectra of the ligand L₁ in methanol.

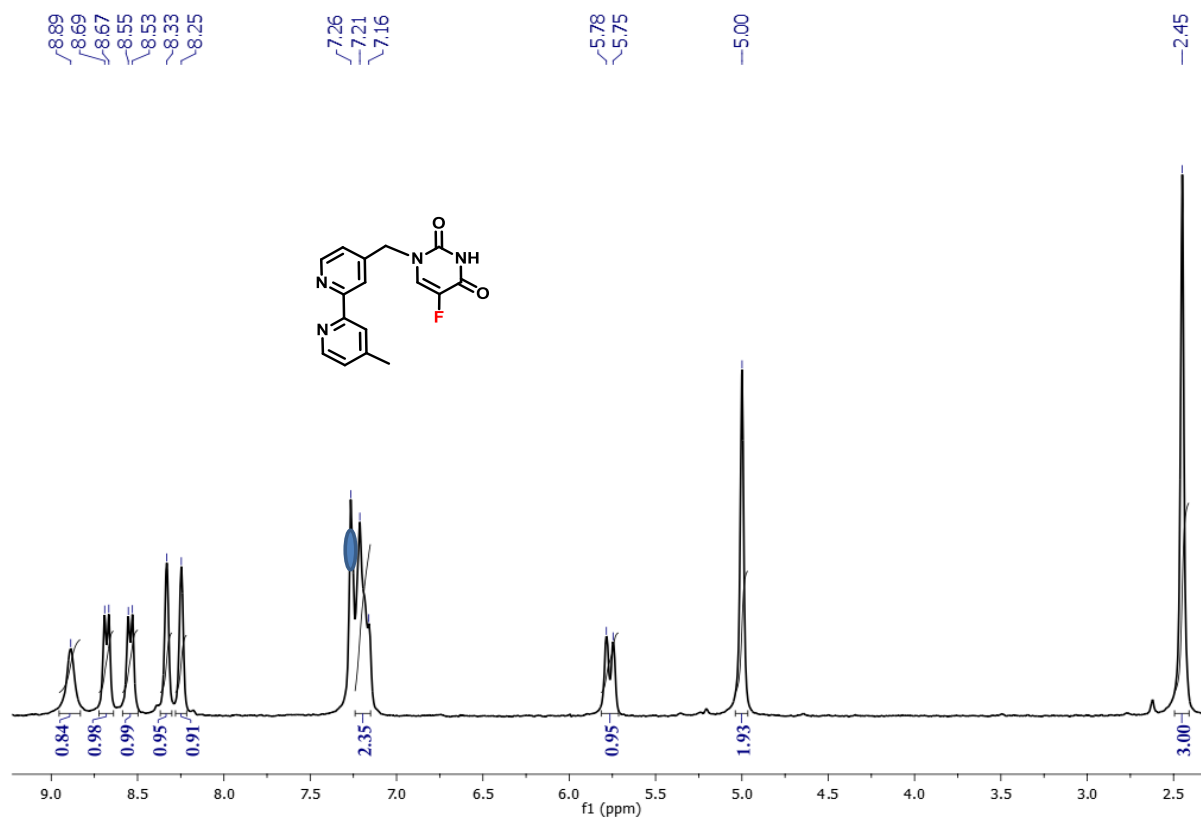


Figure S9. ^1H NMR spectra of the ligand **L₂** recorded in CDCl_3 , the solvent peak was marked in blue circle.

¹⁹F-bpy-5FU

---74.85

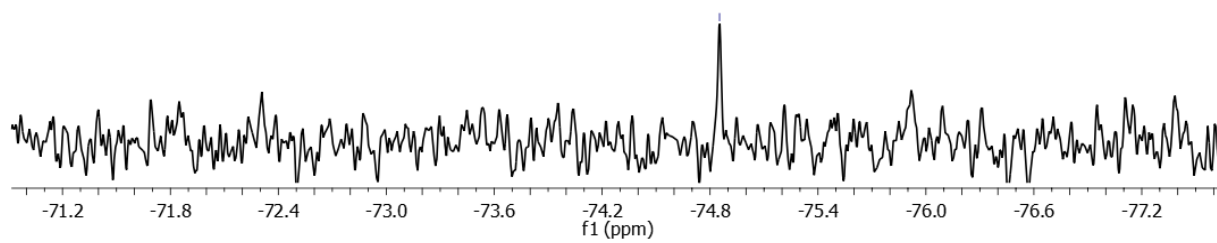
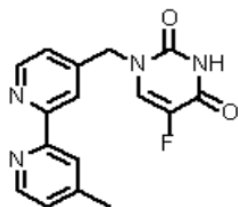


Figure S10. ¹⁹F NMR of the ligand **L**₂ recorded in CDCl₃.

VRB2-37 #8-31 RT: 0.12-0.52 AV: 24 SB: 28 0.00-0.10, 0.61-0.95 NL: 5.53E6
T: (0,0) + c ESI corona sid=80.00 det=1600.00 Full ms [100.00-2000.00]

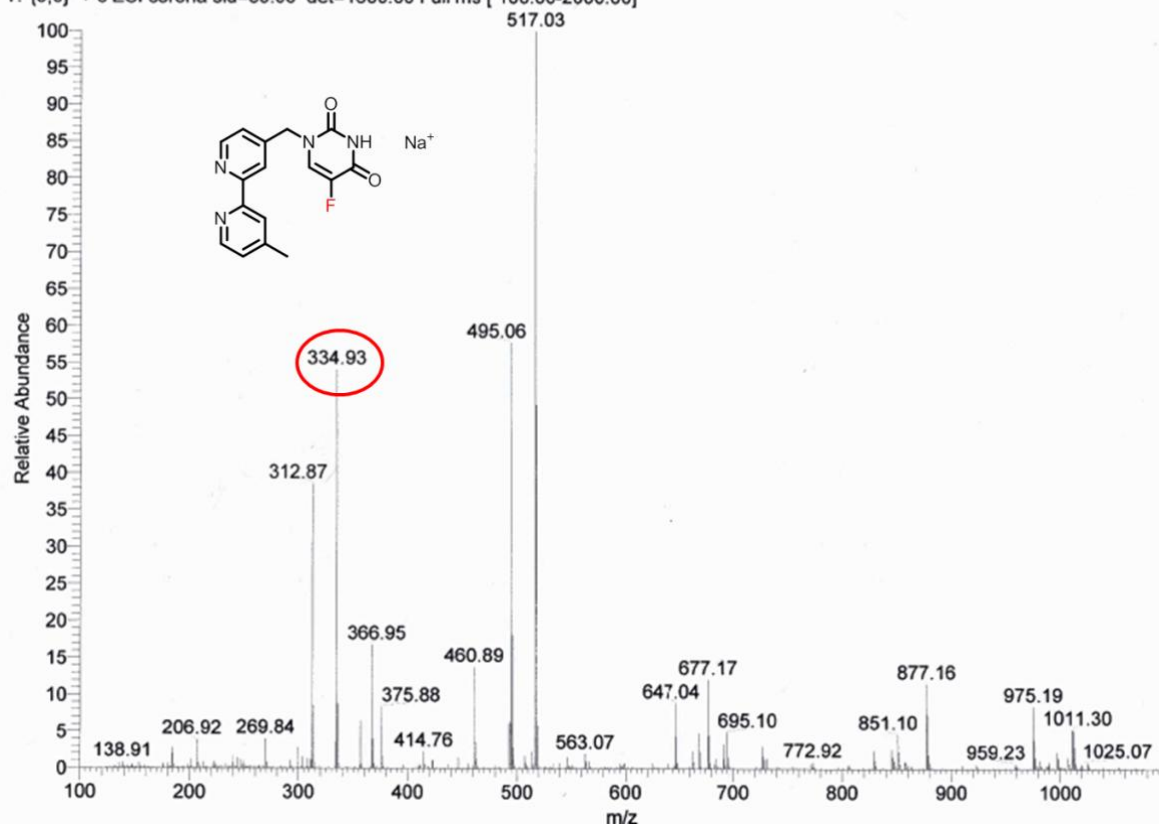


Figure S11. ESI-mass spectra of the ligand L₂ in methanol.

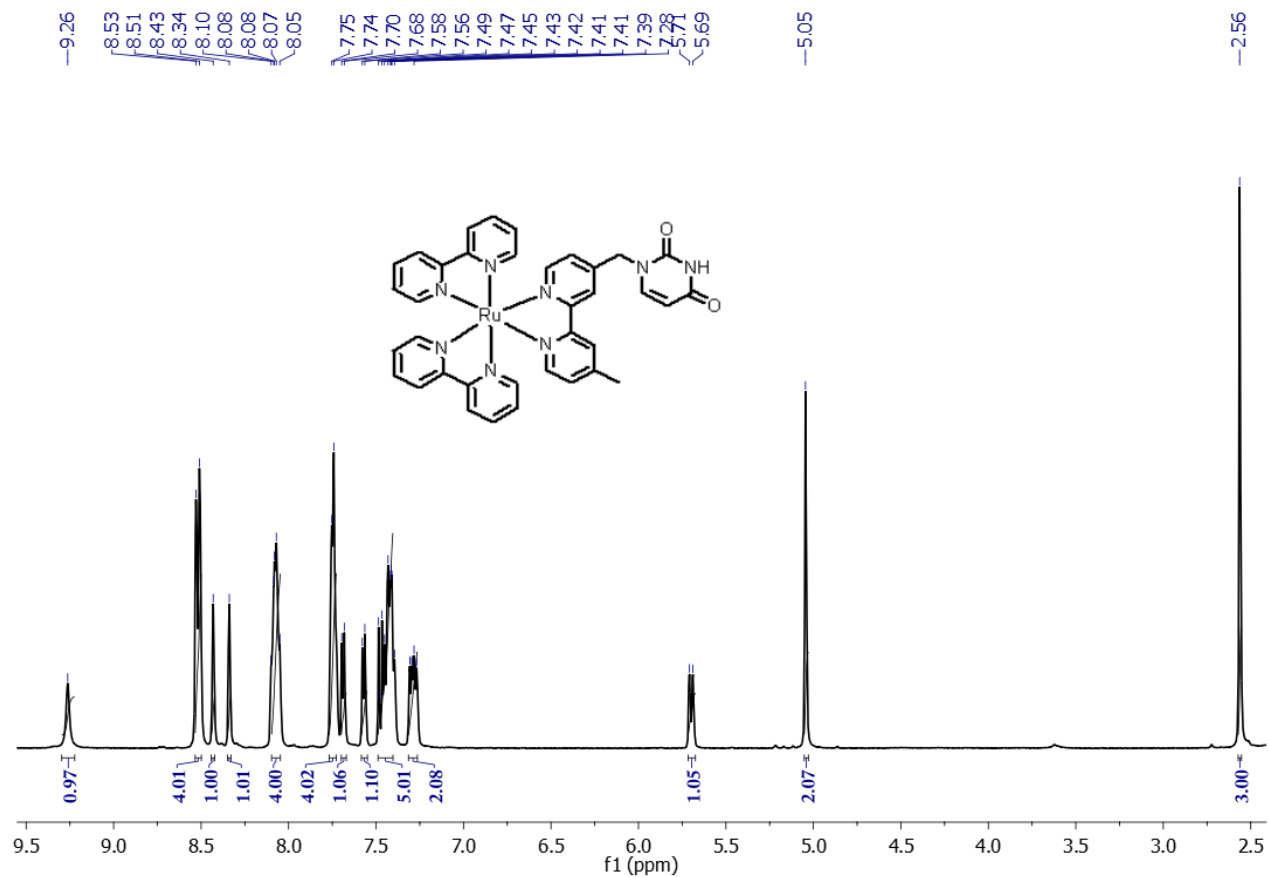


Figure S12. ^1H NMR spectrum for complex **1** recorded in acetonitrile- d_3 .

Ru-uracil #551 RT: 2.45 AV: 1 NL: 4.96E5
T: FTMS + p ESI Full ms [150.00-1000.00]

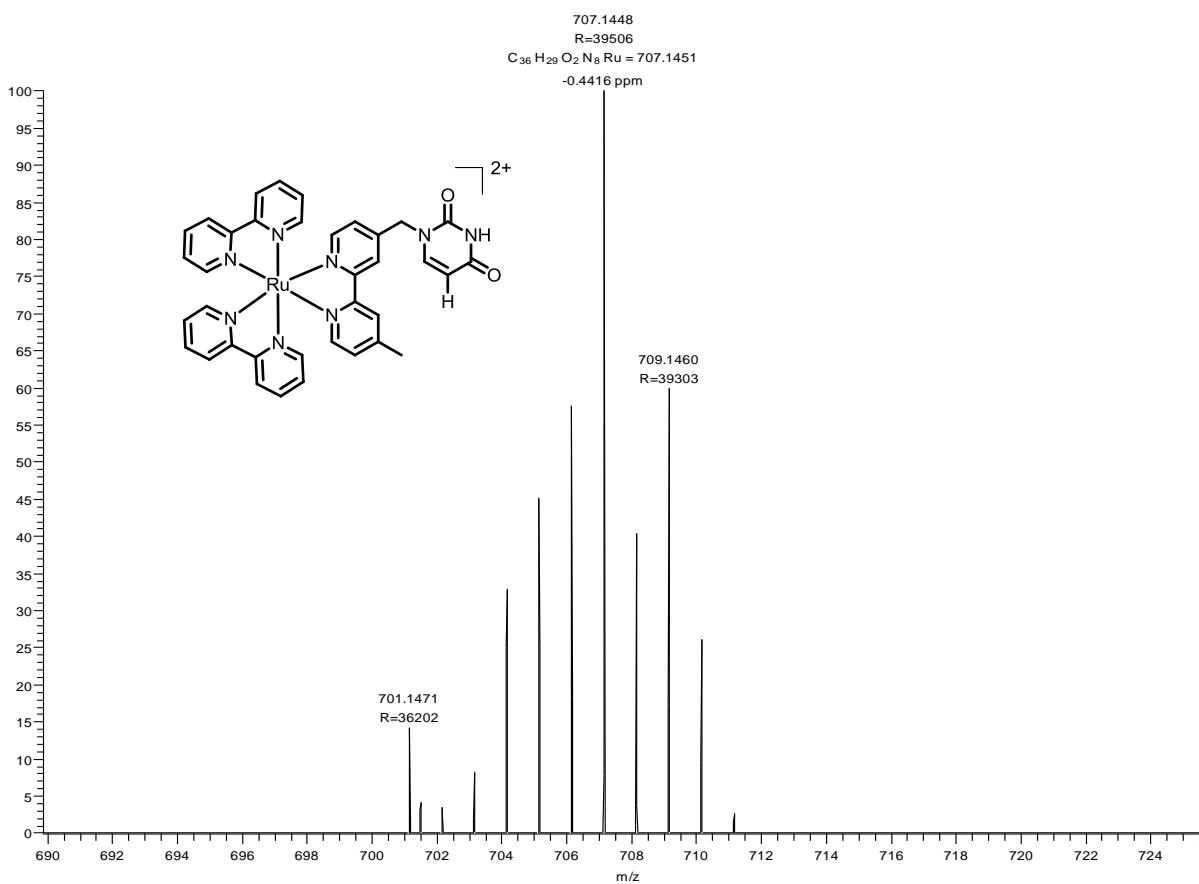


Figure S13. HRMS spectra of complex **1** in acetonitrile.

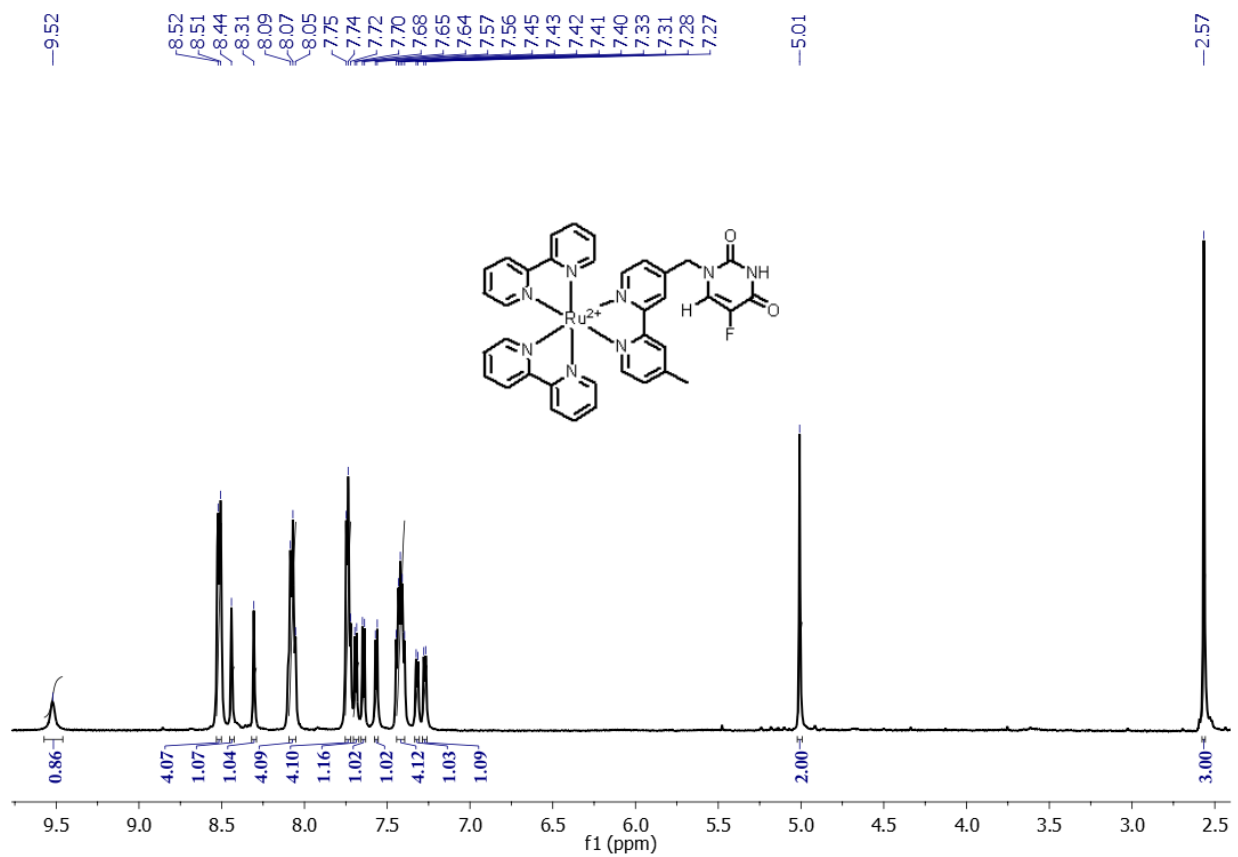


Figure S14. ^1H NMR for the complex **2** recorded in acetonitrile- d_3 .

¹⁹F-NMR

---168.99

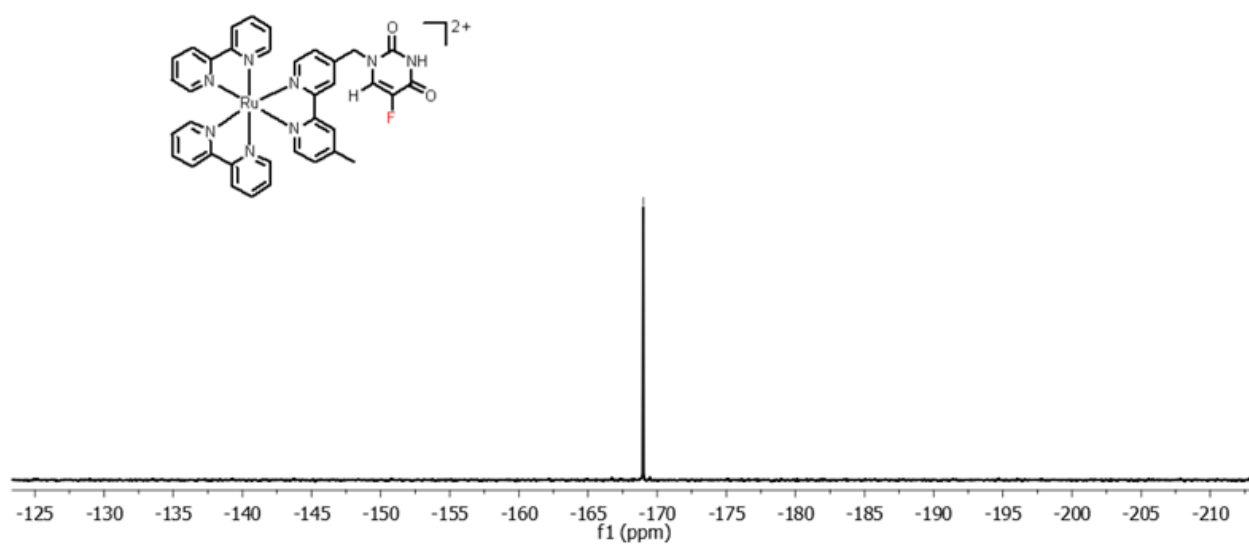


Figure S15. ¹⁹F NMR for the complex **2** recorded in acetonitrile-d₃.

RU-5-FU #397 RT: 1.77 AV: 1 NL: 6.34E7
T: FTMS + p ESI Full ms [100.00-1000.00]

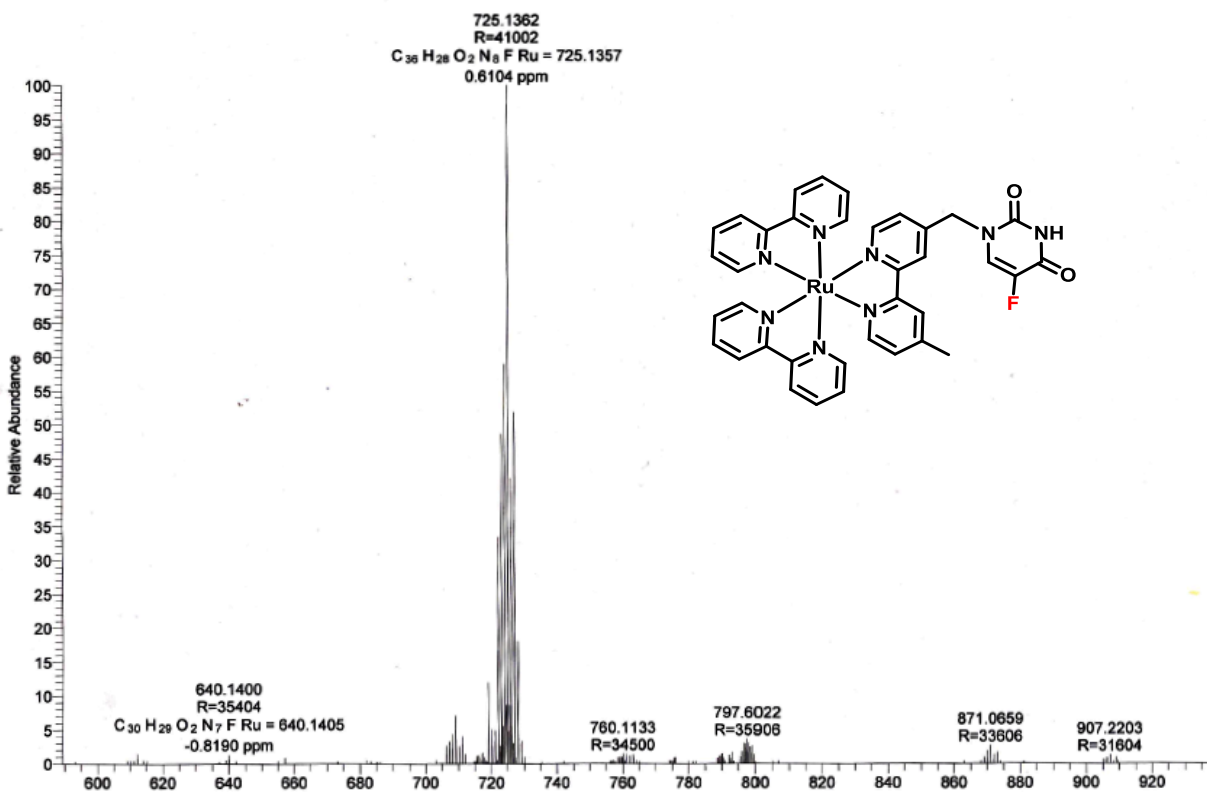


Figure S16. HRMS spectra for the complex **2** in acetonitrile.

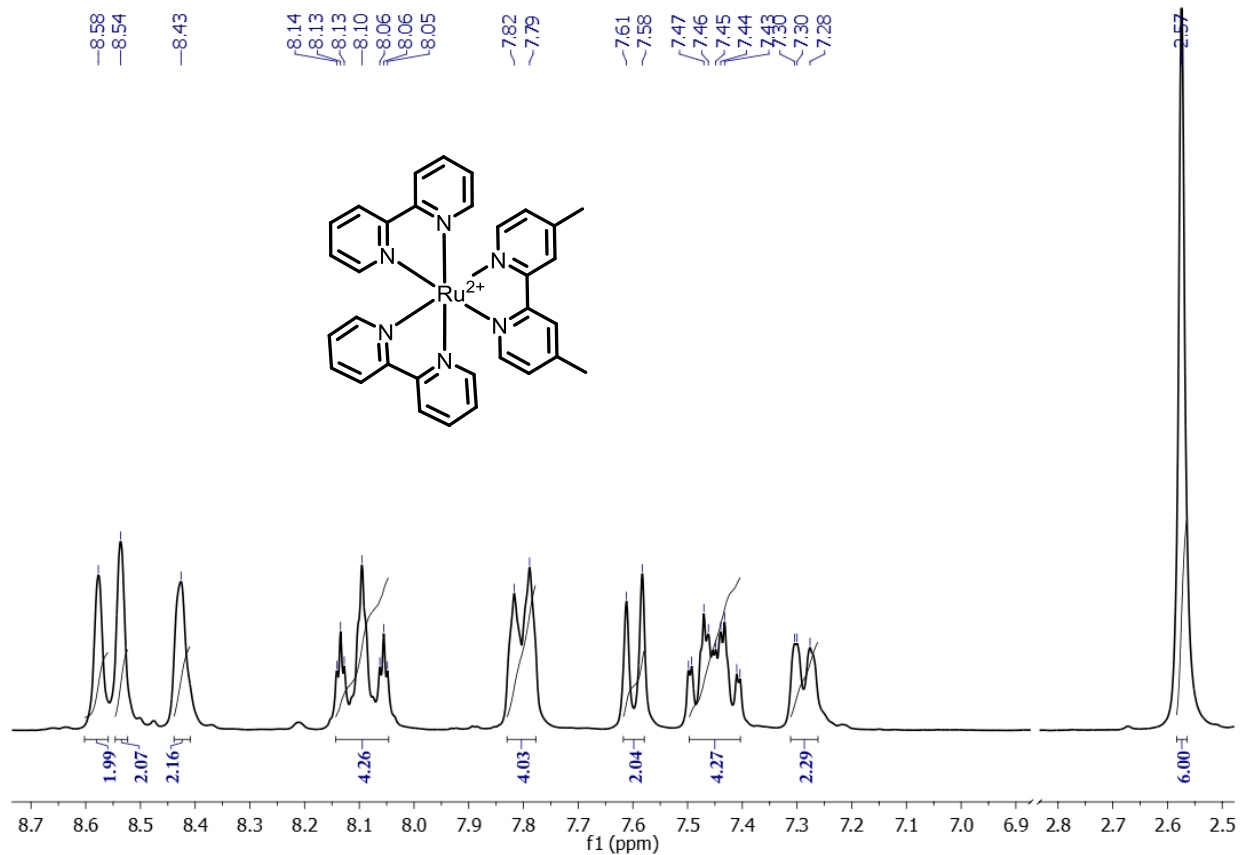


Figure S19. ¹H NMR spectra of complex 3 recorded in acetonitrile-d₃.

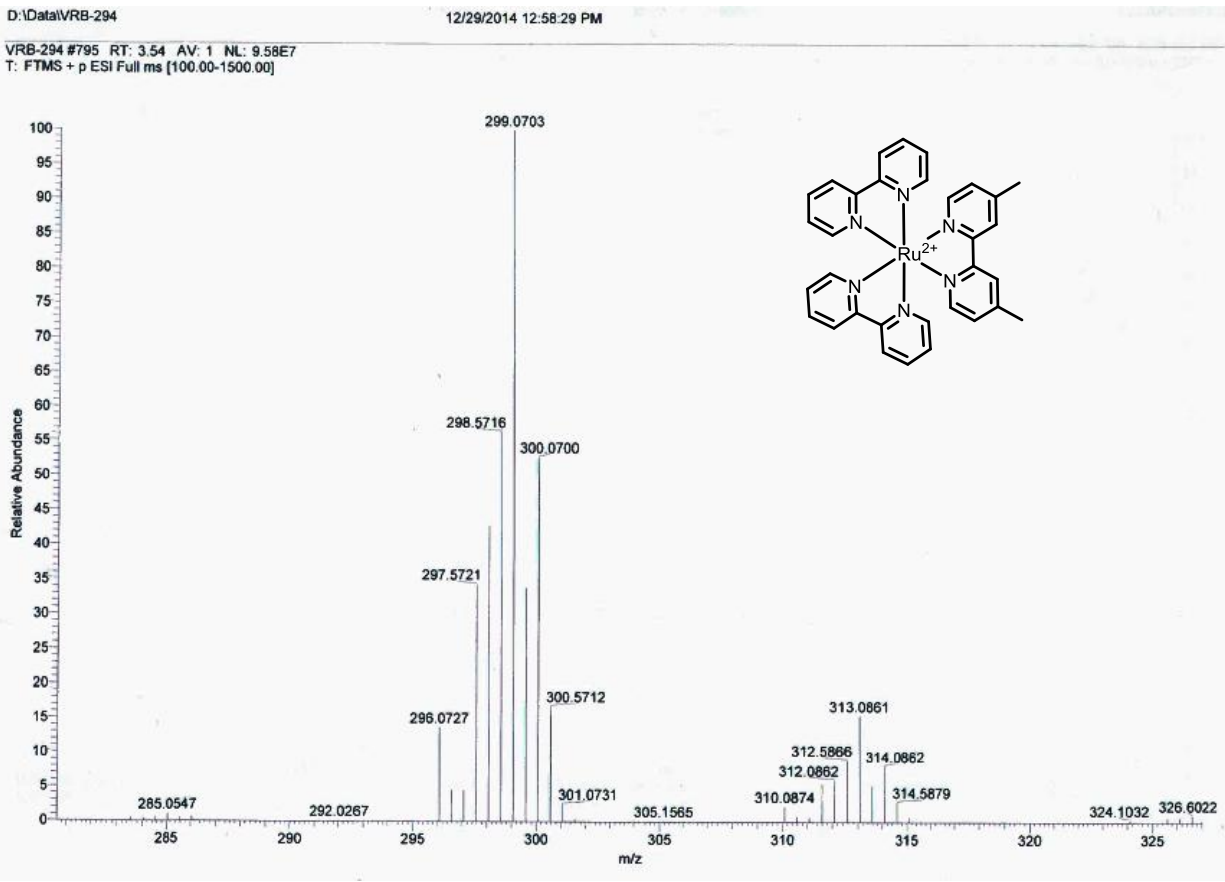


Figure S20: Mass spectra for the complex 3 recorded in acetonitrile.

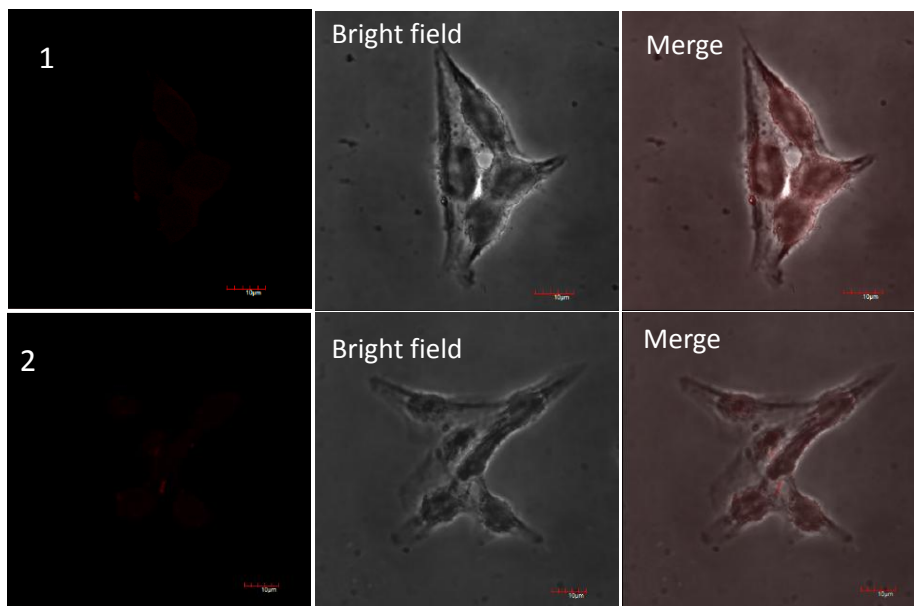


Figure S21. Live MCF-7 cells incubated with **1** and **2** at 4°C for 4h.

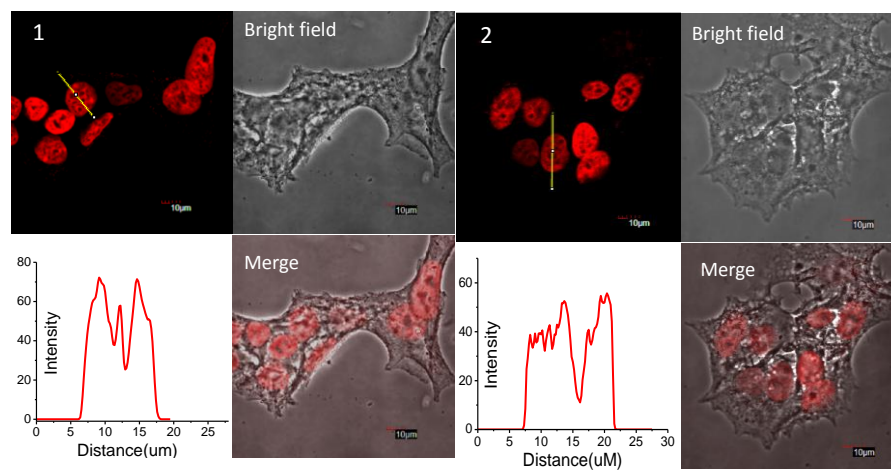


Figure S22. Fixed MCF-7 cells stained with **1** and **2** without DAPI.

References:

1. CrysAlisPro, Version 1.171.33.66; Oxford Diffraction Ltd.: Abingdon, U.K., 2010.
2. G. M. Sheldrick, (1997). SHELXS'97 and SHELXL'97. University of Göttingen, Germany.
3. A. L. Spek (2005) PLATON, A Multipurpose Crystallographic Tool, Utrecht University, Utrecht, The Netherlands.